energies

MDPI

Article

Preliminary Design of Multistage Radial Turbines Based on Rotor Loss Characteristics under Variable Operating Conditions

Zheming Tong [1,2,3,*,†], Zhewu Cheng [1,2,†] and Shuiguang Tong [1,2,*]

[1] State Key Laboratory of Fluid Power and Mechatronic Systems, Zhejiang University, Hangzhou 310027, China
[2] School of Mechanical Engineering, Zhejiang University, Hangzhou 310027, China
[3] Department of Mechanical Engineering, Massachusetts Institute of Technology, Cambridge, MA 02139, USA
* Correspondence: tzm@zju.edu.cn (Z.T.); cetongsg@zju.edu.cn (S.T.)
† These authors contributed equally to this work.

Received: 9 June 2019; Accepted: 28 June 2019; Published: 2 July 2019



Abstract: The loading-to-flow diagram is a widely used classical method for the preliminary design of radial turbines. This study improves this method to optimize the design of radial turbines in the early design phase under variable operating conditions. The guide vane outlet flow angle is a key factor affecting the off-design performance of the radial turbine. To optimize the off-design performance of radial turbines in the early design phase, we propose a hypothesis that uses the ratio of the mean velocity of the fluid relative to the rotor passage with respect to the circumferential velocity of the rotor as an indicator to indirectly and qualitatively estimate the rotor loss, as it plays a key role in the off-design efficiency. Theoretical analysis of rotor loss characteristics under different types of variable operating conditions shows that a smaller design value of guide vane outlet flow angle results in a better off-design performance in the case of a reduced mass flow. In contrast, radial turbines with a larger design value of guide vane outlet flow angle can obtain a better off-design performance with increased mass flow. The above findings were validated with a mean-line model method. Furthermore, this study discusses the optimization of the design value of guide vane outlet flow angle based on the matching of rotor loss characteristics with specified variable operating conditions. It provides important guidance for the design optimization of multistage radial turbines with variable operating conditions in compressed air energy storage (CAES) systems.

Keywords: preliminary design; optimization; rotor loss; guide vane outlet flow angle; radial turbine; CAES

1. Introduction

Multistage radial turbines—usually referring to the multistage radial turbo expanders—are the key component of power generation systems in compressed air energy storage (CAES) and are also employed in the recycling of waste heat, residual pressure, and gas in the petrochemical industry. A schematic diagram of the conventional structure of a multistage radial turbine in CAES systems is shown in Figure 1. It consists of several single-stage radial turbines in separate casings, connected in series. In addition, heat exchangers are connected between stages to preheat the compressed air. Depending on the inlet pressure of the multistage radial turbine, which is generally from 3 to 10 MPa, the number of turbine stages is typically between three and five to ensure that the pressure ratio of each turbine stage falls in the range of two to five. The specific value of the pressure ratio of each turbine stage is related to the turbine inlet temperature. When cold energy production is not required, it is often necessary to meet the requirements of the turbine outlet temperature close to atmospheric temperature. Multistage radial turbines can realize the efficient energy release of a large expansion

ratio from the high pressure of compressed air storage to the atmospheric pressure, and have the advantages of high efficiency, compact structure, and large power capacity. Thus, they are widely used in CAES systems [1,2].

In recent years, CAES technology has received increasing attention as one of the most promising solutions to the problems of intermittency and lack of control in renewable energy generation [3,4]. When multistage radial turbines in CAES systems are integrated with renewable energy generation, the fluctuating power output and inlet pressure make them able to operate under variable working conditions. Guide vane control is a mature and efficient mass flow regulation method that is widely used in turbomachinery. simulation studies have demonstrated the superiority of guide vane control for multistage radial turbines in CAES systems [5–7]. The challenge of multistage radial turbine design thus becomes to maintain high efficiency over a broader range of variable operating conditions involving guide vane opening changes.

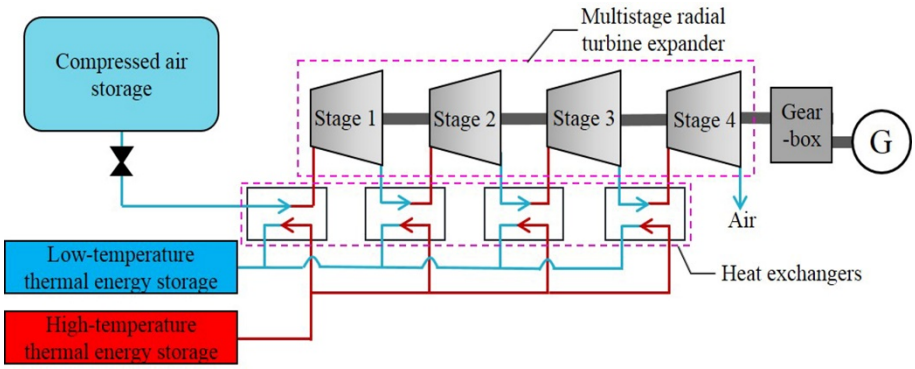


Figure 1. Schematic diagram of a multistage radial turbine in a compressed air energy storage (CAES) system.

As shown in Figure 1, the intermediate turbine duct of the multistage radial turbine is usually a circular pipe in an inter-stage heat exchanger. The pressure change of the internal flow is small, and the flow characteristic is simple. Thus, understanding the internal flow pattern at each turbine stage is more important than that in the intermediate turbine duct between turbine stages. It is the primary factor affecting the performance of multistage radial turbines. Therefore, the design optimization of a single radial turbine stage is still the focus for the design of multistage radial turbines. Computational fluid dynamics (CFD) is the currently preferred method of turbine design optimization, as it enables accurate internal flow analysis to guide the detailed turbine design [8–11]. However, prior to its application, a reasonable one-dimensional preliminary design is the necessary first step in radial turbine design [12–14]. Having such a preliminary design is particularly important for the overall performance analysis of multistage radial turbines.

The loading-to-flow diagram first proposed by Chen and Baines is a classical preliminary design method which has several advantages [15,16]. It relates to the operating conditions of the radial turbine. More importantly, it allows for the creation of a contour map of the expected turbine efficiency, with the loading coefficient and flow coefficient as variables, based on a large amount of data from different radial turbine tests (Figure 2). Thus, it has been widely used for the preliminary design of radial turbines [17–19]. However, the loading-to-flow diagram was developed to achieve an efficient preliminary design of a radial turbine under a single operating condition with fixed geometry. It cannot guarantee an optimal radial turbine design for variable operating conditions, especially with guide vane opening changes. Thus, it is necessary to update the current preliminary design method to meet the needs of variable operating conditions. So far, there has been little public research on this issue apart from the work of Lauriau et al. [20]. They provide some theoretical bases for the preliminary design of variable guide vane geometry-based radial turbines, taking into consideration the need for

multi-point specifications. They also show how the loading-to-flow map can be modified for different optimal target regions.

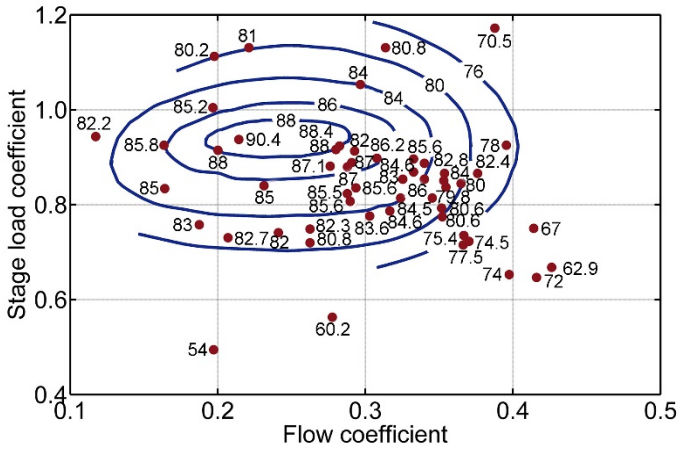


Figure 2. The loading-to-flow diagram [13].

By considering the off-design performance optimization, this paper updates the loading-to-flow diagram method for the preliminary design of radial turbines to accommodate variable operating conditions. The influence of the design value of guide vane outlet flow angle on the rotor loss characteristics was investigated in the continuity of the work presented by Lauriau et al. [20]. Subsequently, aiming at the preliminary design of multistage radial turbines in CAES systems, the optimal design of the guide vane outlet flow angle is discussed from the perspective of the matching of variable operating conditions with rotor loss characteristics. As far as the authors are aware, no similar studies have been performed.

2. Preliminary Design Method Based on the Loading-to-Flow Diagram

According to the definition of the loading-to-flow diagram [17], the loading and flow coefficient can be explained by using the velocity triangles as shown in Figure 3, where the absolute velocity c is a vector addition of the circumferential velocity u and the relative velocity w in the direction of the blade (as a formula: $\vec{c} = \vec{u} + \vec{w}$). The absolute velocity c can be split into a circumferential component c_u and a meridian component c_m. According to Chen and Baines [16], the meridional component of flow velocity at the rotor inlet and outlet can be considered approximately equal. Thus, from Equations (1) and (2), the loading coefficient (ψ) and flow coefficient (ϕ) can be expressed as a function of the guide vane outlet flow angle α_4 and the relative flow angle β_4 at rotor inlet, respectively:

$$\psi = \frac{c_{u4}}{u_4} = \frac{\tan(\alpha_4)}{\tan(\alpha_4) - \tan(\beta_4)}, \tag{1}$$

$$\phi = \frac{c_{m6}}{u_4} \approx \frac{c_{m4}}{u_4} = \frac{1}{\tan(\alpha_4) - \tan(\beta_4)}, \tag{2}$$

where subscripts 4 and 6 denote the rotor inlet and outlet, respectively.

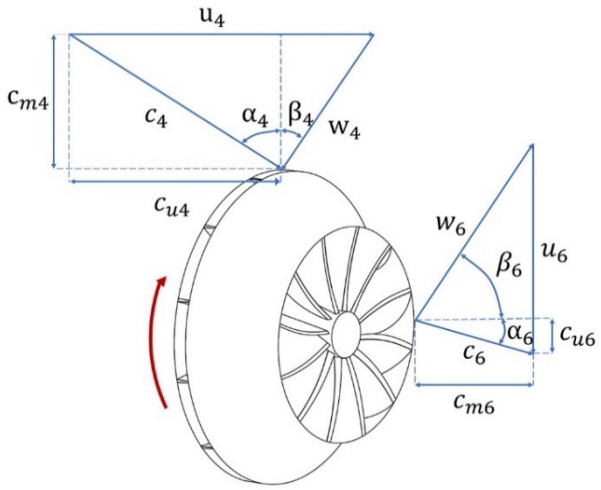


Figure 3. The velocity triangles of the radial turbine rotor inlet and outlet.

The existing literature shows that the optimal values for β_4 are in the range of −40° to −20° [21,22], and the recommended values for α_4 are in the range of 60° to 80° [14]. Thus, by substituting the recommended values of α_4 and β_4 into Equations (1) and (2), the optimum loading-to-flow coefficient range with high expected turbine efficiency could be obtained for the radial turbine preliminary design.

On the other hand, rotor loss is a major factor affecting turbine efficiency, and is directly related to the flow velocity of the fluid in the rotor [23,24]. According to Lauriau et al. [20], the rotor loss can be minimized by reducing the mean velocity of the fluid relative to the rotor passage, which can be expressed as a function of α_4, ϕ, and the mean blade angle at rotor outlet (β_{6m}), as shown in Equation (3). Furthermore, the optimal value of the flow coefficient corresponding to the minimum rotor loss can be expressed by Equation (4).

$$Minimize: \overline{W}_r^2 = \frac{w_4^2 + w_6^2}{2u_4^2} = \frac{1}{2}\phi^2\left(\frac{1}{\cos^2(\alpha_4)} + \frac{1}{\cos^2(\beta_{6m})}\right) + \frac{1}{2} - \phi\tan(\alpha_4), \tag{3}$$

$$\phi_{opt,r} = \frac{\tan(\alpha_4)}{\left(\frac{1}{\cos^2(\alpha_4)} + \frac{1}{\cos^2(\beta_{6m,opt})}\right)}, \tag{4}$$

where $\overline{W}_r$ denotes the ratio of the mean velocity of the fluid relative to the rotor passage with respect to the circumferential velocity of the rotor, $\beta_{6m,opt}$ denotes the recommended values for the mean blade angle at rotor outlet in the range of −60° to −45° [16,25], and w_4 and w_6 denote the relative velocity of air flow at the rotor inlet and outlet, respectively.

Figure 4 depicts the variation of the flow coefficient corresponding to the minimum total loss (corresponding to the optimal values for β_4) and minimum rotor loss (corresponding to the optimal values for $\beta_{6m,opt}$) of the radial turbine as a function of the guide vane outlet flow angle. The former is generally used as the design flow coefficient. It can be seen that the two tended to coincide above a relatively large guide vane outlet angle range ($\alpha_4 \geq 80°$). However, the design flow coefficient significantly increased with the decrease of the guide vane outlet flow angle, but the change of the flow coefficient corresponding to minimum rotor loss was relatively small. The difference between the two gradually increased with the decrease of the guide vane outlet flow angle. Experimental studies have indicated that changes in rotor losses are the most critical factors affecting turbine efficiency under variable operating conditions including pressure ratio change and guide vane opening change [26,27]. It can be inferred that the deviation between the flow coefficient corresponding to minimum rotor loss and the design flow coefficient caused by the different guide vane outlet flow angles will result in different turbine loss characteristics. Therefore, the value of the guide vane outlet flow angle

becomes the key to the preliminary design that aims at optimizing the off-design performance of the radial turbine.

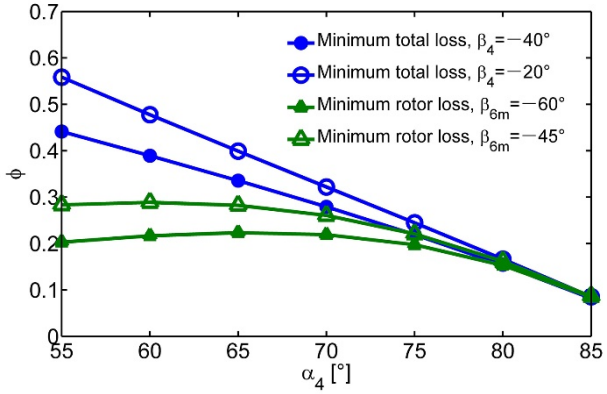


Figure 4. Effect of guide vane outlet flow angle on the optimal flow coefficient value.

3. Analysis of Rotor Loss Characteristics

In this section, the relationship between the design value of guide vane outlet flow angle ($\alpha_{4,d}$) and the rotor loss of the radial turbine is investigated for two typical operating conditions (i.e., variation in pressure ratio and variation in guide vane opening change from the designed value). The ratio of the mean velocity of the fluid relative to the rotor passage with respect to the circumferential velocity of the rotor ($\overline{W}_r$) was determined to infer rotor loss in the early phase of preliminary design without the need of detailed turbine parameters. Since the rotor loss plays a key role in the off-design efficiency of radial turbines, we assumed that $\overline{W}_r$ is a reasonable indictor to qualitatively estimate the rotor loss and turbine efficiency in the preliminary design phase.

3.1. Pressure Ratio Change

For radial turbines with fixed geometry guide vane, the rotor loss under off-design operating conditions is dominated by viscous loss with a nearly constant loss coefficient [24]. Therefore, the value of $\overline{W}_r$ is used to predict the rotor loss characteristics of radial turbines with different $\alpha_{4,d}$ indirectly in the case of pressure ratio change.

In the case where only the change of pressure ratio is considered, the off-design flow coefficient can be estimated using the improved Flügel formula [28] and the definition of flow coefficient (Equation (5)). It can be seen that the off-design flow coefficient is approximately proportional to the pressure ratio change.

$$\begin{cases} \frac{\dot{m}_t}{\dot{m}_{t,d}} = \frac{P_{in}}{P_{in,d}} \sqrt{\frac{1-1/\beta_t^2}{1-1/\beta_{t,d}^2}} \\ \frac{\dot{m}_t}{\dot{m}_{t,d}} = \frac{c_{m6} A_6 \rho_6}{c_{m6,d} A_6 \rho_{6,d}} \approx \frac{(\frac{c_{m6}}{u_4}) \cdot P_6}{(\frac{c_{m6,d}}{u_4}) \cdot P_{6,d}} = \frac{\phi \cdot P_6}{\phi_d \cdot P_{6,d}} \end{cases} \rightarrow \frac{\phi}{\phi_d} \approx \sqrt{\frac{\beta_t^2 - 1}{\beta_{t,d}^2 - 1}}, \quad (5)$$

where $\dot{m}_t$ denotes the mass flow, subscript d denotes the design value, P_{in} denotes the inlet pressure of turbine, β_t denotes the pressure ratio, A_6 denotes the rotor outlet area, ρ_6 denotes the density of gas at the rotor outlet, and P_6 denotes the rotor outlet pressure.

Substituting the off-design flow coefficient into Equation (3), the change characteristics of $\overline{W}_r$ in the case of pressure ratio change could be obtained as shown in Figure 5. The figure shows that for a radial turbine with a small design value of guide vane outlet flow angle (e.g., $\alpha_{4,d} = 60°$), the corresponding $\overline{W}_r$ had a characteristic of decreasing first and then increasing when the pressure ratio was reduced relative to the design point. However, for a radial turbine with a large design value of guide vane outlet flow angle (e.g., $\alpha_{4,d} = 80°$), an increase or decrease in the pressure ratio relative to the design point resulted in an increase in $\overline{W}_r$. The rotor losses also exhibited the characteristics described above due to the change in $\overline{W}_r$. The above results can be explained as follows. For turbines with a small

$\alpha_{4,d}$, the flow coefficient corresponding to minimum rotor loss is less than the design flow coefficient (Figure 4). Therefore, in the process of decreasing the pressure ratio, the off-design flow coefficient (which is approximately proportional to the pressure ratio) is close to the minimum rotor-loss-based flow coefficient first and then gradually deviates from it, resulting in rotor loss exhibiting similar change characteristics. Similarly, for turbines with a large $\alpha_{4,d}$, the flow coefficient corresponding to minimum rotor loss is coincident with the design flow coefficient. An increase or decrease in the pressure ratio will cause the off-design flow coefficient to deviate from the minimum rotor-loss-based flow coefficient, resulting in an increase in rotor loss.

Moreover, within a wide range of pressure ratio change ($0.5 < \beta_{t,i}/\beta_{t,d} < 1.5$), the larger the guide vane outlet flow angle, the smaller $\overline{W}_r$ is. It can be concluded that the turbine efficiency under the same range of pressure ratio change increases proportionally to the design value of guide vane outlet flow angle.

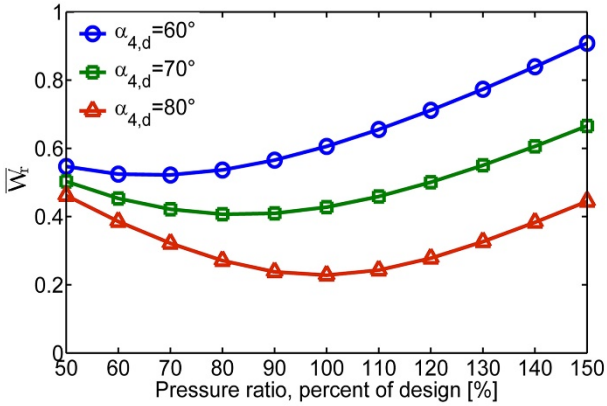


Figure 5. Effect of design guide vane outlet flow angle on the change characteristics of $\overline{W}_r$ under pressure ratio change ($\beta_{6m} = -52.5°$, $\beta_4 = -30°$, $\beta_{t,d} = 3$).

3.2. Guide Vane Opening Change

For radial turbines with variable geometry guide vane, the rotor loss under off-design operating conditions becomes more complex due to the change in the internal flow of the rotor with guide vane opening. Meitner et al. [29] show a relationship between the loss coefficient of rotor kinetic energy and guide vane opening where the loss coefficient increased significantly at small guide vane opening. This occurs because the rotor loss mechanism is not only viscous loss but also increased secondary flow loss at small guide vane opening, according to Otsuka et al. [30]. Therefore, in the case of decreasing guide vane opening (<100% design value), the relative velocity $\overline{W}_r/\overline{W}_{r,d}$ is proposed to indirectly and qualitatively estimate rotor loss for comparison between radial turbines with different design values of guide vane outlet flow angle ($\alpha_{4,d}$). On the other hand, the value of $\overline{W}_r$ is used for increasing guide vane opening (>100% design value).

According to Spence et al. [26,27], the mass flow rate of the radial turbine is approximately proportional to the guide vane opening. As a result, the existing Flügel formula [28] can be updated by multiplying a guide vane opening ratio (O_r) to estimate the mass flow rate under guide vane opening change. From the updated Flügel formula and the definition of flow coefficient, the off-design flow coefficient can be obtained as shown in Equation (6).

$$\begin{cases} \frac{\dot{m}_t}{\dot{m}_{t,d}} \approx O_r \frac{P_{in}}{P_{in,d}} \sqrt{\frac{1-1/\beta_t^2}{1-1/\beta_{t,d}^2}} \\ \frac{\dot{m}_t}{\dot{m}_{t,d}} = \frac{c_{m6} A_6 \rho_6}{c_{m6,d} A_6 \rho_{6,d}} \approx \frac{(\frac{c_{m6}}{u_4}) \cdot P_6}{(\frac{c_{m6,d}}{u_4}) \cdot P_{6,d}} = \frac{\phi \cdot P_6}{\phi_d \cdot P_{6,d}} \end{cases} \rightarrow \frac{\phi}{\phi_d} \approx O_r \sqrt{\frac{\beta_t^2 - 1}{\beta_{t,d}^2 - 1}}, \quad (6)$$

where O_r is defined as the ratio of the off-design guide vane opening to the design value.

Moreover, from the guide vane geometric (Figure 6), a sinus rule can be employed to estimate the updated α_4 caused by the guide vane opening change as shown in Equation (7) [23]. Finally, by substituting the off-design flow coefficient and the updated α_4 into Equation (3), the off-design $\overline{W}_r$ the corresponding $\overline{W}_r/\overline{W}_{r,d}$ can be obtained.

$$\alpha_4 = \cos^{-1}(\frac{O}{S}) = \cos^{-1}(\frac{O}{O_d} \times \frac{O_d}{S}) = \cos^{-1}(O_r \cdot \cos(\alpha_{4,d})), \tag{7}$$

where O denotes the guide vane opening and S denotes the span of the guide vane at the outlet.

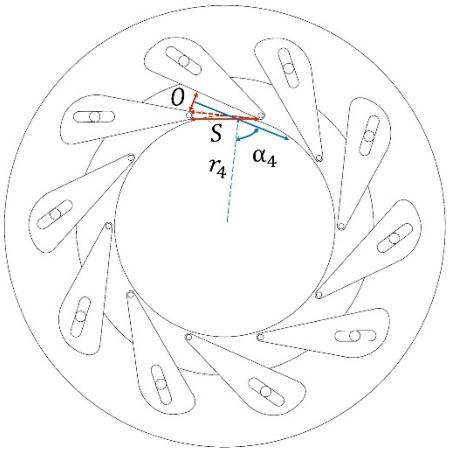


Figure 6. Typical variable-geometry guide vanes for radial turbines.

From Equation (6), the variation in flow coefficient was closely related to the pressure ratio in the case of guide vane opening change. Thus, the rotor loss analysis of two representative cases of guide vane opening change was carried out respectively; these were the constant pressure ratio case and a more complicated case where the pressure ratio changed inversely to the guide vane opening.

Figure 7a shows that in the case where the pressure ratio remained constant, $\overline{W}_r/\overline{W}_{r,d}$ decreased significantly as the guide vane opening decreased. Although the difference between different $\alpha_{4,d}$ was not notable, it can be seen that the $\overline{W}_r/\overline{W}_{r,d}$ of the radial turbine with a smaller $\alpha_{4,d}$ was smaller, which means a smaller increase in the rotor loss with decreased guide vane opening. In the case where the guide vane opening was increased, the larger the $\alpha_{4,d}$, the smaller the $\overline{W}_r$. This means a smaller increase in the rotor loss with the increased guide vane opening. The above results can be explained as follows. In the case of a constant pressure ratio, the flow coefficient is proportional to the guide vane opening ratio (Equation (6)). Since smaller $\alpha_{4,d}$ leads to a larger corresponding design flow coefficient (Figure 4), it can be inferred that the relative velocity of air flow at the rotor inlet (w_4) is also larger (Figure 3). Thus, within the same regulation range of the guide vane opening, the changes in w_4 caused by the flow coefficient change are more pronounced in both the increasing and decreasing directions. This directly leads to a more significant change in the rotor loss.

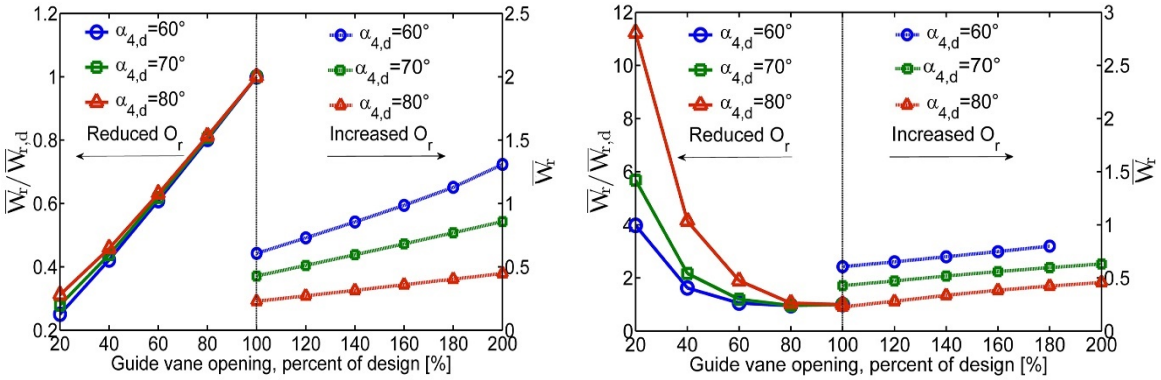


Figure 7. Effect of design guide vane outlet flow angle on the change characteristics of $\overline{W}_r$ with variable guide vane opening: (**a**) constant pressure ratio; (**b**) constant flow coefficient ($\beta_{6m} = -52.5°$, $\beta_4 = -30°$).

Figure 7b shows that in the case where the pressure ratio changed inversely with the guide vane opening and maintained a constant flow coefficient, $\overline{W}_r/\overline{W}_{r,d}$ increased significantly as the guide vane opening decreased. In contrast, the radial turbine with smaller $\alpha_{4,d}$ had a smaller increase in $\overline{W}_r/\overline{W}_{r,d}$, which means a relatively smaller increase in the rotor loss with decreased guide vane opening. In the case where the guide vane opening was increased, the larger the $\alpha_{4,d}$, the smaller the $\overline{W}_r$. This means a smaller increase in the rotor loss with the increased guide vane opening. The above results can be explained as follows. According to Figure 4, the larger α_4, the more obvious the change (decreased) of the flow coefficient corresponding to the minimum rotor loss. Thus, for the radial turbine with a smaller $\alpha_{4,d}$, the deviation of the off-design flow coefficient (approximately equal to the design value) from the flow coefficient (decreased) corresponding to the minimum rotor loss caused by the decrease of the guide vane opening is smaller. It can also be inferred that the increase in the rotor loss would be smaller. In contrast, in the case where the guide vane opening was increased, the increased flow coefficient corresponding to the minimum rotor loss tended to be gentle with the increase of α_4. The deviation of the off-design flow coefficient (approximately equal to the design value) from the flow coefficient (increased) corresponding to the minimum rotor loss caused by the increase of the guide vane opening can be ignored for radial turbines with a different $\alpha_{4,d}$. Therefore, due to the smaller $\overline{W}_r$ at the design point, the larger the $\alpha_{4,d}$, the smaller the off-design rotor loss.

Furthermore, by comparing Figure 7a,b, we can find that the inverse change of pressure ratio with the change in the guide vane opening will increase the rotor loss in the case of reduced guide vane opening. On the contrary, it can mitigate the increase of the rotor loss in the case of increased guide vane opening.

In conclusion, the difference in the rotor loss characteristics under guide vane opening change for radial turbines with different $\alpha_{4,d}$ is determined by the directionality of the guide vane regulation. It can be concluded that the optimum design of the guide vane outlet flow angle is closely related to the directionality of the guide vane regulation.

4. Optimal Design of the Guide Vane Outlet Flow Angle for Multistage Radial Turbines

This section presents a discussion of the optimal design of the guide vane outlet flow angle ($\alpha_{4,d}$) for a multistage radial turbine from the perspective of matching the rotor loss characteristics with variable operating conditions. In addition, the multistage radial turbine of a CAES pilot plant named "TICC-500" [31] was taken as an example for analysis (Table 1).

Table 1. Parameters of the multistage turbine in a "TICC-500" CAES pilot system [31].

Turbine Stage	Input Pressure, MPa	Outlet Pressure, MPa
High-Pressure Turbine (HP)	2.50	1.13
Medium-Pressure Turbine (MP)	1.12	0.40
Low-Pressure Turbine (LP)	0.39	0.10

To obtain the representative variable operating conditions of the multistage radial turbine based on guide vane control, only the case of regulating the guide vane opening of the high-pressure turbine stage was considered here. Since the rotational speed of the multistage radial turbine in a CAES system is generally constant, the mass flow rate of each turbine stage under guide vane control can be estimated by the updated Flügel formula in Equation (6), which includes a guide vane opening ratio (O_r). On this basis, to solve the operating conditions of each turbine stage in the multistage radial turbine at a certain inlet pressure and guide vane opening, the pressure ratios were updated to iteratively calculate the mass flow for each turbine stage until the continuity of mass flow was met. Furthermore, by substituting off-design the operating conditions (guide vane opening and pressure ratio) into Equation (6), the corresponding the flow coefficient could be obtained.

Depending on the directivity of the guide vane opening regulation, the case where the guide vane opening is reduced and increased with respect to the design value is defined as a down-regulation and an up-regulation, respectively. Figure 8a,b presents the variable operating conditions of the multistage radial turbine in the case of down-regulation and up-regulation, respectively. We assumed steady-state operation conditions with different guide vane openings, and the hysteresis during continuous down- and up-regulation was not considered in this study.

(1) Down-Regulation of the Guide Vane Opening

When the inlet pressure of the multistage radial turbine is high while the load demand is low, the down-regulation of the guide vane opening is conducted to reduce the mass flow rate. Figure 8a shows that the pressure ratio of the low-pressure (LP) turbine decreased significantly with the decrease of the guide vane opening of the high-pressure (HP) turbine and relatively small change in the expansion ratio of the medium-pressure (MP) turbine. In contrast, the pressure ratio of the HP turbine changed inversely to the guide vane opening, which significantly increased with the decrease of the guide vane opening.

(2) Up-Regulation of the Guide Vane Opening

When the inlet pressure of the multistage radial turbine is relatively low while the load demand is high, the up-regulation of the guide vane opening is conducted to increase the mass flow rate. Figure 8b shows that the pressure ratio of the LP turbine increased significantly with the increase of the guide vane opening of the HP turbine, while the expansion ratio of the MP turbine remained almost constant. Like the down-regulation of the guide vane opening, the pressure ratio of HP turbine changed inversely to the guide vane opening, which reduced significantly with the increase of the guide vane opening.

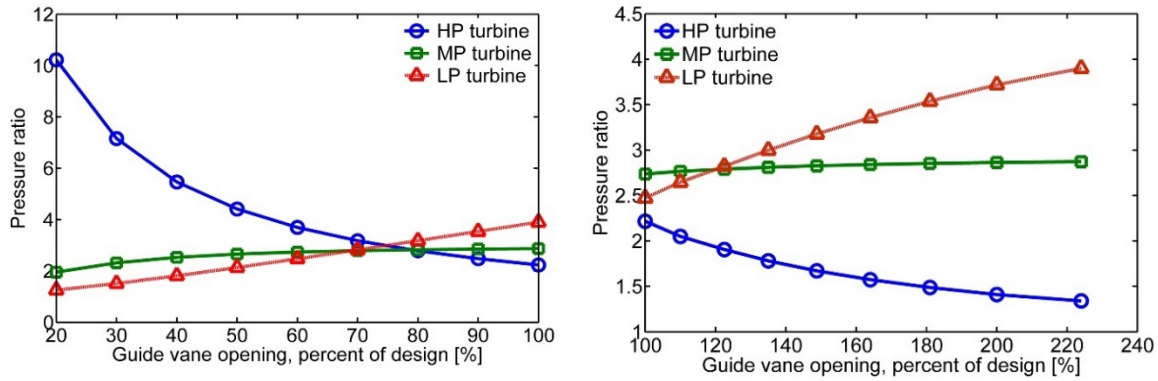


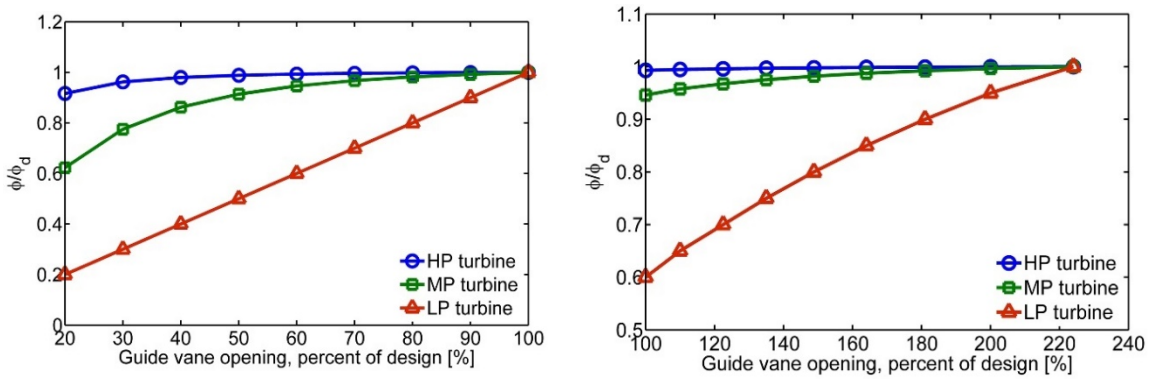
Figure 8. Variable operating conditions for a multistage radial turbine under guide vane opening change: (**a**) down-regulation at rated inlet pressure; (**b**) up-regulation at 60% the rated inlet pressure.

Figure 9a,b presents the flow coefficient variation characteristics of the multistage radial turbine under the variable operating conditions shown in Figure 8a,b, respectively. Combined with the findings regarding the relationship of off-design performance versus the design value of the guide vane outlet flow angle ($\alpha_{4,d}$) for the radial turbine shown in Section 3, the recommendations for the optimum $\alpha_{4,d}$ in the preliminary design of the multistage radial turbine are as follows.

i. The variable operating condition of the LP turbine belongs to the expansion ratio change, and the flow coefficient varies notably within a range smaller than the design value. According to the findings on the relationship of off-design performance versus $\alpha_{4,d}$ for radial turbines under pressure ratio change (Section 3.1), a larger $\alpha_{4,d}$ should be used for the LP turbine to achieve better off-design performance. A value of approximately 80° is recommended.

ii. The variable operating condition of the MP turbine also belongs to the expansion ratio change, but the flow coefficient varies within a small range that is less than the design value. Therefore, turbine efficiency under design conditions dominates the performance of the MP turbine under variable operating conditions. As a result, a larger $\alpha_{4,d}$ should be used for the MP turbine (i.e., about 80°).

iii. The variable operating condition of the HP turbine is a complicated case where the pressure ratio changes inversely with the guide vane opening and maintains a nearly constant flow coefficient. According to the findings on the relationship of off-design performance versus $\alpha_{4,d}$ for radial turbines under guide vane opening change (Section 3.2), the optimum $\alpha_{4,d}$ mainly depends on the direction of the guide vane opening changes relative to the design point. For a multistage radial turbine in a CAES system with constant air storage pressure, the inlet pressure of the HP turbine stage remains at the rated value, so only the down-regulation of the guide vane opening is performed. Accordingly, a smaller $\alpha_{4,d}$ should be used for the HP turbine stage to achieve better off-design performance. Further considering the influence of design efficiency on off-design performance, the recommended design values are in the range of 70–75°. For a multistage radial turbine in a CAES system with varying air storage pressure, the inlet pressure of the HP turbine stage varies with air storage pressure, so there is a simultaneous need for up- and down-regulation of the guide vane opening. In this case, it is necessary to comprehensively consider the influence of the rotor loss characteristics and design efficiency on the off-design performance in determining $\alpha_{4,d}$.



(**a**) (**b**)

Figure 9. Flow coefficient variation for the multistage turbine under guide vane opening change: (**a**) down-regulation at rated inlet pressure; (**b**) up-regulation at 60% of the rated inlet pressure.

5. Case Study and Discussion

In this section, we compare the off-design performance of a group of radial turbines with different design values of guide vane outlet flow angle. To ensure the comparability of different radial turbine performances, the preliminary design results of radial turbine obtained under the same design conditions were employed for the case study. Moreover, the performance evaluation of the radial turbine was conducted using the mean-line model method.

The mean-line model method previously developed in our group is a proven performance evaluation method for radial turbines. Since the model evaluation of radial turbines is not the focus of this study, please refer to one of our previous publications for more details [7]. The model uses limited turbine geometry information to predict the turbine performance under variable operating conditions, which is especially valuable in the preliminary design process. The total-to-static efficiency of the radial turbine was calculated by the specific work output, isentropic enthalpy drops, and turbine losses, as shown in Equation (8). According to the Euler equation of turbomachines [32], the specific work output can be calculated with Equation (9). Table 2 gives the loss model combination suitable for the turbine loss evaluation under variable guide vane opening, which involves four types of main turbine losses: stator loss, incidence loss, rotor loss, and exit loss.

$$\eta_{t-s} = \frac{W_t}{\Delta h_{1-6s}} = \frac{\Delta h_{1-6s} - \sum h_{loss}}{\Delta h_{1-6s}}, \tag{8}$$

$$W_t = u_4 c_{u4} - u_6 c_{u6}, \tag{9}$$

where W_t denotes the specific work output of the radial turbine, Δh_{1-6s} denotes the isentropic enthalpy drop between the guide vane inlet and rotor outlet, and h_{loss} denotes the turbine loss.

Table 2. The loss model combination of the radial turbine.

Loss	Reference	Model
Stator Loss	[33]	$\Delta h_{stator} = \frac{1}{2} K_n {c_{3s}}^2$
Incidence Loss	[29]	$\Delta h_{incidence} = \frac{1}{2} {w_4}^2 (1 - \cos^n i)$
Rotor Loss	[29]	$\Delta h_{rotor} = \frac{1}{2} K_r ({w_4}^2 \cos^2 i + {w_6}^2)$
Exit Loss	[24]	$\Delta h_{exit} = \frac{1}{2} {c_{m6}}^2$

The design conditions of the radial turbines in this case study are shown in Table 3. Based on the conclusions of the matching analysis in Section 4, three typical design values of guide vane outlet flow angle ($\alpha_{4,d}$= [70°; 75°; 80°]) were employed for the case study. The main parameters of the radial turbines were obtained by a preliminary design algorithm proposed by Ventura et al. [17] (Table 4).

Table 3. The design conditions of the radial turbines for the case study.

Parameter	Value
Inlet Temperature, K	430
Inlet Total Pressure, MPa	10.00
Outlet Pressure, MPa	3.33
Mass Flow Rate, kg/s	24.80

Table 4. The preliminary design results of the radial turbines for the case study.

Parameter	Case A	Case B	Case C
Guide Vane Outlet Flow Angle, degree	70	75	80
Loading Coefficient	0.78	0.82	0.88
Flow Coefficient	0.28	0.23	0.16
Rotor			
Rotational Speed, r/min	50112	39620	32329
Inlet Radius, mm	73.5	90.8	107.0
Inlet Tip Width, mm	8.6	9.3	11.7
Inlet Relative Flow Angle, degree	−38.5	−40.6	−38.2
Blade Number	11	15	18
Outlet Tip Radius, mm	21.1	24.1	29.0
Outlet Hub Radius, mm	52.1	59.6	72.0
Outlet Blade Angle, degree	−62.3	−66.4	−73.2
Stator			
Inlet Radius, mm	99.0	119.4	138.8
Throat Width, mm	11.7	8.4	5.2
Vane height, mm	8.6	9.3	11.7
Outlet Radius, mm	79.2	95.5	111.0
Blade Number	14	18	23
Performance			
Total-to-Static Efficiency	0.881	0.895	0.899

Figure 10 presents the performance curves of radial turbines with different design values of guide vane outlet flow angle operating under pressure ratio change. It can be seen that the larger the design value of guide vane outlet flow angle, the higher the design efficiency of the radial turbine, and the higher the efficiency operating under variable pressure ratio in a certain range ($0.5 < \beta_{t,i}/\beta_{t,d} < 1.5$). These are consistent with the findings of the rotor loss characteristic analysis under pressure ratio change (Section 3.1). It should also be noted that the turbine efficiency deteriorated significantly as the pressure ratio decreased to less than about 60% of the design value. However, simply optimizing the design value of the guide vane outlet angle did not seem to be effective in improving this deterioration.

Figure 11a,b, gives the performance curves of two typical cases of guide vane opening change: the constant pressure ratio case and the constant flow coefficient case. First, it can be seen that the radial turbines with different design values of guide vane outlet flow angle had significant differences in the distribution of the efficient operating range under guide vane opening changes, which verifies the finding of the rotor loss characteristic analysis in Section 3.2. Specifically, the radial turbine with a larger design value of guide vane outlet flow angle (e.g., $\alpha_{4,d} = 80°$) had a broader efficient operating range (e.g., turbine efficiency > 0.8) and higher efficiency for the up-regulation of the guide vane opening, while a smaller design value of guide vane outlet flow angle resulted in broader efficient operating range and higher efficiency for the down-regulation of the guide vane opening. Furthermore, comparing Figure 11a,b, it can be found that the deterioration of the turbine efficiency under the down-regulation of the guide vane opening could be alleviated by reducing the reverse increase in the pressure ratio versus the guide vane opening change. Similarly, for the up-regulation of the guide vane opening, when the design value of the guide vane outlet flow angle was large, diminishing the inverse reduction of the pressure ratio could improve the turbine efficiency. However, for a turbine with

a smaller design value of guide vane outlet flow angle (e.g., $\alpha_{4,d} = 70°$), this could worsen efficiency. These are also consistent with the findings in Section 3.2.

Based on the above, for a multistage radial turbine that simultaneously needs up- and down-regulation of the guide vane opening, the design value of guide vane outlet flow angle for the high-pressure turbine stage (or other turbine stages with variable geometry guide vane) is recommended to be about 80°. In this case, higher design efficiency and wide efficient operating range for the up-regulation can be obtained, while the turbine efficiency deterioration under down-regulation can be improved with combined control of the guide vane openings of the multistage radial turbine. The combined control of the guide vane openings of the multistage radial turbine has been proved to be able to alleviate the reverse change in pressure ratio versus the guide vane opening [6]. This could be an effective way to achieve optimum performance for a multistage radial turbine operating under variable working conditions.

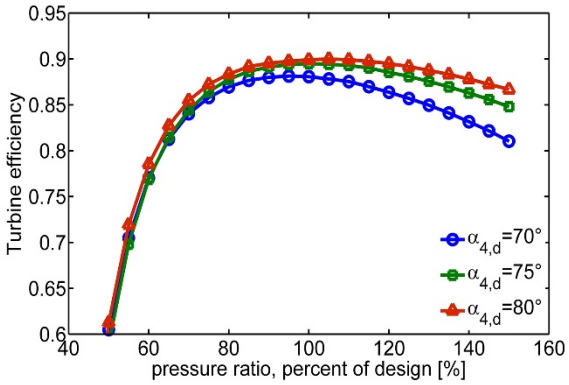


Figure 10. Turbine performance under pressure ratio change.

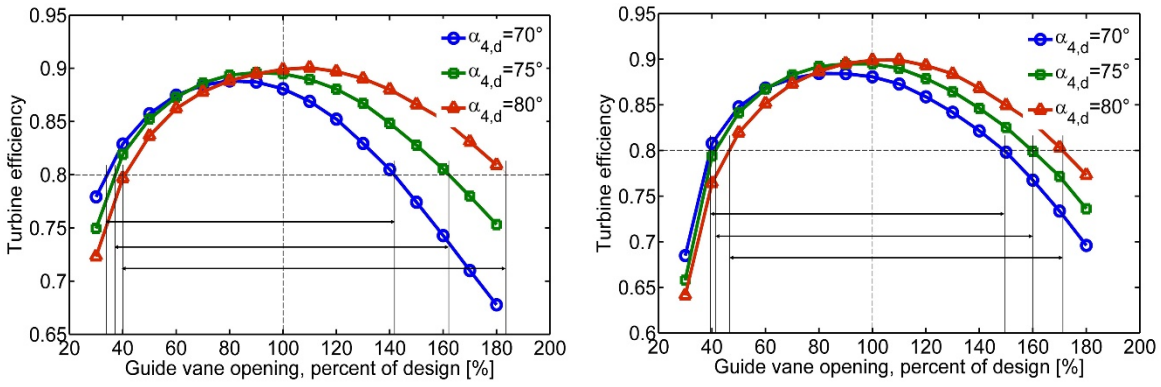


Figure 11. Turbine performances when the guide vane opening changes and: (**a**) the pressure ratio is constant; (**b**) the pressure ratio changes inversely to the guide vane opening.

6. Conclusions

This study improves the classical loading-to-flow diagram method to meet the design needs of radial turbines with variable operating conditions. To optimize the off-design performance of radial turbines in the early design phase, we proposed a hypothesis that uses the ratio of the mean velocity of the fluid relative to the rotor passage with respect to the circumferential velocity of the rotor as an indicator to indirectly and qualitatively estimate the rotor loss, as it plays a key role in the off-design efficiency. This hypothesis is based on the findings from existing studies indicating that rotor loss is a function of the flow velocity within the rotor.

The findings of off-design rotor loss analysis for radial turbines with a different design value of guide vane outlet flow angle are as follows:

(1) For a radial turbine with a smaller design value of guide vane outlet flow angle, the rotor loss first decreased and then increased with the decrease of mass flow. This means better off-design performance in the case of reducing the mass flow. This applies both under conditions of pressure ratio change and of guide vane opening change. However, due to a higher rotor loss at design conditions, the turbine efficiency under pressure ratio changes may be lower than for radial turbines with a larger guide vane outlet flow angle.

(2) A radial turbine with a larger design value of guide vane outlet flow angle not only had higher efficiency at design conditions but also had better off-design performance in the case of increased mass flow. This held for changes in both pressure ratio and guide vane opening.

The above findings were validated with the mean-line model method [7]. Furthermore, based on the findings, this study discusses the optimization of the design value of guide vane outlet flow angle based on the matching of rotor loss characteristics with specified variable operating conditions for a multistage radial turbine in a compressed air energy storage system. It provides important guidance for the design optimization of multistage radial turbines operating under variable working conditions.

Author Contributions: Conceptualization, Z.C., Z.T., and S.T.; Methodology, Z.C.; Formal analysis, Z.C.; Validation, Z.C.; Writing, Z.C. and Z.T.; Supervision, S.T. and Z.T.

Funding: We would like to acknowledge the National Key R&D Program of China (2018YFB0606105), National Natural Science Foundation of China (51708493), Zhejiang Provincial Natural Science Foundation (LR19E050002), Zhejiang Province Key Science and Technology Project (2018C01020, 2018C01060, 2019C01057), and the Youth Funds of State Key Laboratory of Fluid Power & Mechatronic Systems (SKLoFP_QN_1804).

Conflicts of Interest: The authors declare no conflict of interest.

References

1. He, W.; Wang, J.; Ding, Y. New radial turbine dynamic modelling in a low-temperature adiabatic compressed air energy storage system discharging process. *Energy Convers. Manag.* **2017**, *153*, 144–156. [CrossRef]
2. Tong, S.; Cheng, Z.; Cong, F.; Tong, Z.; Zhang, Y. Developing a grid-connected power optimization strategy for the integration of wind power with low-temperature adiabatic compressed air energy storage. *Renew. Energy* **2018**, *125*, 73–86. [CrossRef]
3. Venkataramani, G.; Parankusam, P.; Ramalingam, V.; Wang, J. A review on compressed air energy storage—A pathway for smart grid and polygeneration. *Renew. Sustain. Energy Rev.* **2016**, *62*, 895–907. [CrossRef]
4. Argyrou, M.C.; Christodoulides, P.; Kalogirou, S.A. Energy storage for electricity generation and related processes: Technologies appraisal and grid scale applications. *Renew. Sustain. Energy Rev.* **2018**, *94*, 804–821. [CrossRef]
5. Li, H.; Li, W.; Liu, D.; Zhang, X.; Zhu, Y.; Chen, H. Effect of adjustable guide vanes on the characteristic of multistage reheating radial inflow turbine. *Proc. CSEE* **2016**, *36*, 6180–6186.
6. Liu, D.; Li, W.; Li, H.; Zhang, X.; Zhu, Y.; Chen, H. Characteristic analysis of combined regulation of adjustable guide vanes of multistage radial inflow turbines. *Energy Storage Sci. Technol.* **2017**, *6*, 1286–1294.
7. Cheng, Z.; Tong, S.; Tong, Z. Bi-directional nozzle control of multistage radial-inflow turbine for optimal part-load operation of compressed air energy storage. *Energy Convers. Manag.* **2019**, *181*, 485–500. [CrossRef]
8. Li, P.; Han, Z.; Jia, X.; Mei, Z.; Han, X. Analysis of the effects of blade installation angle and blade number on radial-inflow turbine stator flow performance. *Energies* **2018**, *11*, 2258. [CrossRef]
9. Capata, R.; Hernandez, G. Preliminary design and simulation of a turbo expander for small rated power Organic Rankine Cycle (ORC). *Energies* **2014**, *7*, 7067–7093. [CrossRef]
10. Tong, Z.; Li, Y.; Westerdahl, D.; Adamkiewicz, G.; Spengler, J.D. Exploring the effects of ventilation practices in mitigating in-vehicle exposure to traffic-related air pollutants in China. *Environ. Int.* **2019**, *127*, 773–784. [CrossRef]
11. Tong, Z.; Chen, Y.; Malkawi, A. Defining the Influence Region in neighborhood-scale CFD simulations for natural ventilation design. *Appl. Energy* **2016**, *182*, 625–633. [CrossRef]
12. Daabo, A.M.; Al Jubori, A.; Mahmoud, S.; Al-Dadah, R.K. Development of three-dimensional optimization of a small-scale radial turbine for solar powered Brayton cycle application. *Appl. Therm. Eng.* **2017**, *111*, 718–733. [CrossRef]

13. Fiaschi, D.; Innocenti, G.; Manfrida, G.; Maraschiello, F. Design of micro radial turboexpanders for ORC power cycles: From 0D to 3D. *Appl. Therm. Eng.* **2016**, *99*, 402–410. [CrossRef]
14. Rahbar, K.; Mahmoud, S.; Al-Dadah, R.K. Mean-line modeling and CFD analysis of a miniature radial turbine for distributed power generation systems. *Int. J. Low Carbon Technol.* **2016**, *11*, 157–168. [CrossRef]
15. Chen, H.; Baines, N.C. Analytical Optimization Design of Radial and Mixed Flow Turbines. *Proc. Inst. Mech. Eng. Part A J. Power Energy* **1992**. [CrossRef]
16. Chen, H.; Baines, N.C. The aerodynamic loading of radial and mixed-flow turbines. *Int. J. Mech. Sci.* **1994**, *36*, 63–79. [CrossRef]
17. Ventura, C.A.M.; Jacobs, P.A.; Rowlands, A.S.; Petrie-Repar, P.; Sauret, E. Preliminary design and performance estimation of radial inflow turbines: An automated approach. *J. Fluid Eng. Trans. ASME* **2012**, *134*, 31102. [CrossRef]
18. Shao, S.; Deng, Q.H.; Feng, Z.P. An automated approach for the radial inflow turbine preliminary design and off-design prediction. *J. Eng. Thermophys.* **2016**, *37*, 67–71.
19. Da Silva, E.R.; Kyprianidis, K.G.; Säterskog, M.; Camacho, R.G.R.; Sarmiento, A.L.E. Preliminary design optimization of an organic Rankine cycle radial turbine rotor. In Proceedings of the ASME Turbo Expo, Charlotte, NC, USA, 26–30 June 2017. [CrossRef]
20. Lauriau, P.T.; Binder, N.; Carbonneau, X.; Cros, S.; Roumeas, M. Preliminary design considerations for variable geometry radial turbines with multi-points specifications. In Proceedings of the 12th European Conference on Turbomachinery Fluid Dynamics and Thermodynamics (ETC 2017), Stockholm, Sweden, 3–7 April 2017.
21. Woolley, N.H.; Hatton, A.P. Viscous Flow in Radial Turbomachine Blade Passages. In Proceedings of the Conference on Heat and Fluid Flow in Steam and Gas Turbine Plant, London, UK, 3–5 April 1974; pp. 175–181.
22. Spence, S.W.T.; Artt, D.W. An experimental assessment of incidence losses in a radial inflow turbine rotor. *Proc. Inst. Mech. Eng. Part A J. Power Eng.* **1998**. [CrossRef]
23. Moustapha, H.; Zelesky, M.F.; Japiske, D.; Baines, N.C. *Axial and Radial Turbines*; Concepts NREC: White River Junction, VT, USA, 2003.
24. Suhrmann, J.F.; Peitsch, D.; Gugau, M.; Heuer, T.; Tomm, U. Validation and development of loss models for small size radial turbines. In Proceedings of the ASME Turbo Expo, Glasgow, UK, 14–18 June 2010. [CrossRef]
25. Qiu, X.; Baines, N. Performance prediction for high pressure-ratio radial inflow turbines. In Proceedings of the ASME Turbo Expo, Montreal, QC, Canada, 14–17 May 2007. [CrossRef]
26. Spence, S.W.T.; Artt, D.W. Experimental performance evaluation of a 99.0 mm radial inflow nozzled turbine with different stator throat areas. *Proc. Inst. Mech. Eng. Part A J. Power Eng.* **1997**. [CrossRef]
27. Spence, S.W.T.; Doran, W.J.; Artt, D.W. Experimental performance evaluation of a 99.0 mm radial inflow nozzled turbine at larger stator-rotor throat area ratios. *Proc. Inst. Mech. Eng. Part A J. Power Eng.* **1999**. [CrossRef]
28. Zhang, N.; Cai, R. Analytical solutions and typical characteristics of part-load performances of single shaft gas turbine and its cogeneration. *Energy Convers. Manag.* **2002**, *43*, 1323–1337. [CrossRef]
29. Meitner, P.L.; Glassman, A.J. *Off-Design Performance Loss Model for Radial Turbines with Pivoting, Variable-Area Stators*; NASA TP-1708; NASA: Washington, DC, USA, 1980.
30. Otsuka, K.; Komatsu, T.; Tsujita, H.; Yamaguchi, S.; Yamagata, A. Numerical analysis of flow in radial turbine (Effects of nozzle vane angle on internal flow). *Int. J. Fluid Mach. Syst.* **2016**, *9*, 137–142. [CrossRef]
31. Wang, S.; Zhang, X.; Yang, L.; Zhou, Y.; Wang, J. Experimental study of compressed air energy storage system with thermal energy storage. *Energy* **2016**, *103*, 182–191. [CrossRef]
32. Dixon, S.; Hall, C. *Fluid Mechanics and Thermodynamics of Turbomachinery*; Elsevier Ltd.: Amsterdam, The Netherlands, 2010.
33. Glassman, A.J.; Center, L.R. *Computer Program for Design Analysis of Radial-Inflow Turbines*; NASA TN D-9164; NASA: Washington, DC, USA, 1976.



© 2019 by the authors. Licensee MDPI, Basel, Switzerland. This article is an open access article distributed under the terms and conditions of the Creative Commons Attribution (CC BY) license (http://creativecommons.org/licenses/by/4.0/).